Available online at www.sciencedirect.com

SCIENCE DIRECT®

Tectonophysics 394 (2004) 21–40

TECTONOPHYSICS

www.elsevier.com/locate/tecto

The record of historic earthquakes in lake sediments of Central Switzerland

Katrin Monecke[a,b,*], Flavio S. Anselmetti[a], Arnfried Becker[b], Michael Sturm[c], Domenico Giardini[b]

[a]*Geological Institute, ETH Zürich, Sonneggstr. 5, Zürich 8092, Switzerland*
[b]*Geophysical Institute, ETH Hönggerberg, Zürich 8093, Switzerland*
[c]*Sedimentology Section, Department of Surface Waters (SURF), EAWAG, Dübendorf 8600, Switzerland*

Received 19 November 2003; accepted 19 July 2004
Available online 12 October 2004

Abstract

Deformation structures in lake sediments in Central Switzerland can be attributed to strong historic earthquakes. The type and spatial distribution of the deformation structures reflect the historically documented macroseismic intensities thus providing a useful calibration tool for paleoseismic investigations in prehistoric lake sediments.

The Swiss historical earthquake catalogue shows four moderate to strong earthquakes with moment magnitudes of M_w=5.7 to M_w=6.9 and epicentral intensities of I_0=VII to I_0=IX that affected the area of Central Switzerland during the last 1000 years. These are the 1964 Alpnach, 1774 Altdorf, 1601 Unterwalden, and 1356 Basel earthquakes. In order to understand the effect of these earthquakes on lacustrine sediments, four lakes in Central Switzerland (Sarner See, Lungerer See, Baldegger See, and Seelisberg Seeli) were investigated using high-resolution seismic data and sediment cores. The sediments consist of organic- and carbonate-rich clayey to sandy silts that display fine bedding on the centimeter to millimeter scale. The sediments are dated by historic climate and environmental records, ^{137}Cs activity, and radiocarbon ages. Deformation structures occur within distinct zones and include large-scale slumps and rockfalls, as well as small-scale features like disturbed and contorted lamination and liquefaction structures. These deformations are attributed to three of the abovementioned earthquakes. The spatial distribution of deformation structures in the different lakes clearly reflects the historical macroseismic dataset: Lake sediments are only affected if they are situated within an area that underwent groundshaking not smaller than intensity VI to VII. We estimate earthquake size by relating the epicentral distance of the farthest liquefaction structure to earthquake magnitude. This relationship is in agreement with earthquake size estimations based on the historical dataset.
© 2004 Elsevier B.V. All rights reserved.

Keywords: Historic earthquakes; Paleoseismology; Lake deposits; Central Switzerland

* Corresponding author. Tel.: +41 1 632 3698; fax: +41 1 632 1030.
E-mail address: katrin.monecke@erdw.ethz.ch (K. Monecke).

0040-1951/$ - see front matter © 2004 Elsevier B.V. All rights reserved.
doi:10.1016/j.tecto.2004.07.053

1. Introduction

Although the instrumental record of northern Switzerland shows relatively low levels of seismicity, the historic earthquake record of the last 1000 years indicates several damaging earthquakes with moment magnitudes of $M_w \geq 5$ and epicentral intensities of $I_0 \geq$VII [Earthquake Catalogue of Switzerland (ECOS), Fäh et al., 2003; intensities after European Macroseismic Scale (EMS)]. The largest known events are the 1356 Basel and the 1601 Unterwalden earthquakes with magnitudes of M_w=6.9 and M_w=6.2 and intensities of I_0=IX and I_0=VII, respectively (uncertainty bounds on historic earthquakes are estimated at ±0.5 magnitude units and ±0.5–1.0 intensity units). Triggered in an area with a low seismicity level and a long seismic cycle, these strong earthquakes are considered to have recurrence intervals of hundreds to thousands of years. The historic earthquake record is thus not long enough to determine the frequency of large magnitude events. Therefore, geological archives have to be investigated in order to get reliable data about seismic hazard and risk. Lake deposits are regarded as most suitable for paleoseismic studies as they often form a detailed and continuous environmental archive (Ricci Lucchi, 1995). Sims (1973, 1975) observed that earthquake-induced deformation structures in lake sediments could be correlated to major historic earthquakes. Traces of prehistoric earthquakes were described in different lacustrine environments (e.g., Ringrose, 1989; Marco et al., 1996). Using small-scale soft sediment deformation structures, it was also possible to estimate paleoearthquake size (e.g., Rodriguez Pascua et al., 2000, 2003; Ringrose, 1989; Davenport, 1994). In modern lakes, paleoseismic studies focused mainly on earthquake-generated slump deposits using seismic data (Shilts and Clague, 1992; Chapron et al., 1999). In Vierwaldstätter See in Central Switzerland, several slump deposits were related to historic earthquakes as well as to prehistoric events (Siegenthaler and Sturm, 1991; Siegenthaler et al., 1987; Schnellmann et al., 2002).

Within this study, we will show the effect of strong historic earthquakes on lacustrine deposits in order to develop a calibration scheme for paleoseismic investigations in prehistoric lake sediments. Four lakes in Central Switzerland with different sedimentary processes distributed within an area of 2000 km^2 were investigated using high-resolution reflection seismic data and sediment cores. Deformation structures, identified both in the seismic lines and sediment cores, are described and dated. Special emphasis has been placed on small-scale in situ deformation structures in sediment cores as they allow estimations of local ground shaking intensities. The sedimentary data are compared to the historical macroseismic dataset in order to calibrate the observed structures: different deformation structures in varying distances to the epicenters are related to corresponding macroseismic intensities. Earthquake size is calculated from the epicentral distance of the farthest liquefaction structure and compared to the historical dataset.

2. Historical seismicity

The historical ECOS shows two centers of enhanced seismicity north of the Alpine range: the Basel region and the region of Central Switzerland (Fäh et al., 2003) (Fig. 1A). The Basel region belongs to the Cenozoic rift system of the Upper Rhine Graben. The instrumentally measured recent seismicity (since 1975) has been relatively weak, including a major M_w=4.9 event north of Basel (July 15, 1980—Plaine de Haute Alsace, Habsheim; Fäh et al., 2003). The preinstrumental macroseismic earthquake catalogue covering approximately the last 1000 years, however, shows that the Basel region was affected by at least three to four larger earthquakes with magnitudes of $M_w \geq 5$ and epicentral intensities of $I_0 \geq$VII. This includes the October 18, 1356 earthquake of Basel, which is the largest known earthquake in Central Europe with M_w=6.9 and I_0=IX. Investigations of recent earthquakes in the Basel region indicate relatively shallow hypocentral depths located between 5 and 15 km below the surface (Deichmann et al., 2000; Bonjer, 1997). Calculated focal mechanisms of some larger earthquakes show a predominance of strike–slip faults and normal faults with ENE–WSW direction of extension.

The seismically active area of Central Switzerland is located at the northern Alpine front. In this region, seismic activity since 1975 has been extremely low, showing one larger event in Iberg of November 16, 1995 with a magnitude of M_w=4.0 (Fäh et al., 2003;

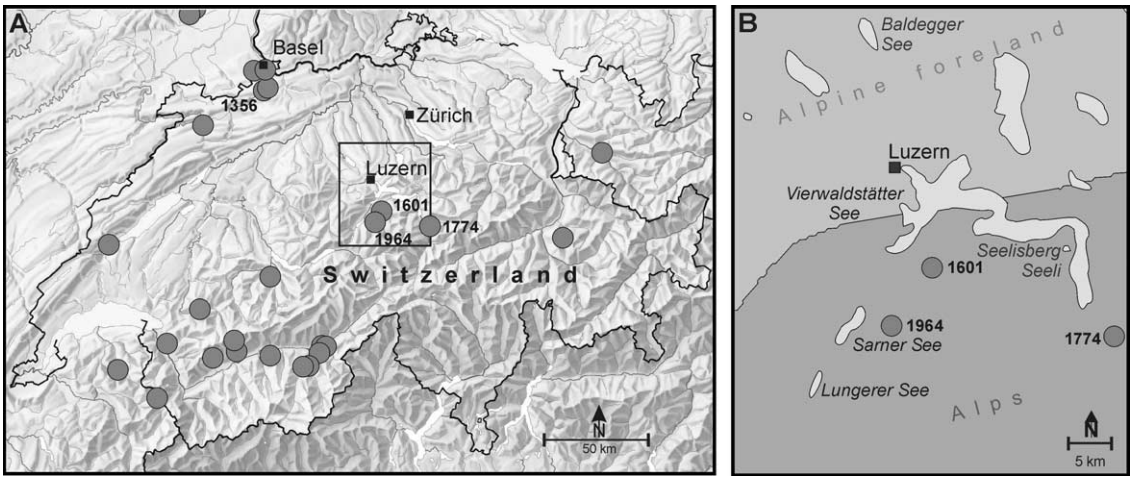

Fig. 1. (A) Historical seismicity in Switzerland and surrounding areas. Dots mark epicenters of historic earthquakes of the last 1000 years with moment magnitudes M_w>5.4 (after Fäh et al., 2003). (B) Location of studied lakes.

Deichmann et al., 2000). In contrast, the preinstrumental macroseismic dataset in Central Switzerland indicates a relatively high seismicity with five larger earthquakes ($M_w \geq 5$ and $I_0 \geq$VII), including the 1964 Alpnach, 1774 Altdorf, and 1601 Unterwalden earthquakes. The 1601 Unterwalden earthquake, with a magnitude of M_w=6.2 and intensity of I_0=VII, is supposed to be one of the largest events in Switzerland.

Instrumentally registered recent earthquakes show remarkably shallow hypocentral depths, indicating that earthquake activity takes place within the sedimentary cover (Deichmann et al., 2000). Although focal mechanisms were difficult to determine, there are indications that steeply dipping, N–S-trending, strike–slip faults obliquely cut the WSW–ENE-striking Alpine structures (Ahorner et al., 1972; Schindler, 1980).

3. Methods

Prior to coring, all lakes were subjected to a high-resolution seismic survey (3.5 kHz pinger source) to determine the bathymetry of the lake basin as well as the 3D architecture and stratigraphy of sedimentary units. Based on the seismic dataset, coring sites were determined. Short cores of 1–2 m in length were taken with a gravity corer. Long cores up to 14 m long were taken from three lakes using either the Kullenberg or UWITEC piston coring system (Kelts et al., 1986). The long sediment cores were cut into roughly 1-m-long pieces. All cores were logged using a GEOTEK multiscanner to obtain petrophysical data (p-wave velocity and amplitude, bulk density, and magnetic susceptibility). Afterwards, the cores were split lengthwise into two halves and photographed immediately after opening. They were described sedimentologically and sampled for smearslide analyses and dating.

4. Dating of sediments

The correlation of earthquake-induced deformations to historic earthquakes has to be based on careful dating of the sediments and the development of an accurate time frame of the sedimentary record. The most exact dating can be achieved by correlation of historically reported events to changes in the sedimentary record of the lake. Historical documents of local municipal and cantonal offices were examined for large flood events, anthropogenic lake level regulations, or river diversions. Furthermore, a compilation of historical climate data of Switzerland encompassing the last 500 years was used (Pfister, 1999). Remarkable periods of hot, cold, wet, or dry conditions were correlated to changes in the sedimentary record.

Two radiometric dating methods were used: determination of ^{137}Cs activity in the youngest sedi-

ments and radiocarbon dating in the older deposits. The artificial fission product ^{137}Cs was injected into the atmosphere during nuclear weapon tests since 1952 AD reaching peak concentrations in 1963 AD and during the catastrophic Chernobyl accident in 1986 AD. ^{137}Cesium activity was measured at each centimeter at the EAWAG (Swiss Federal Institute for Environmental Science and Technology) using GELI borehole detectors. Measuring time was 24 h per sample.

Ideal samples for radiocarbon dating are terrestrial macrofossils such as leaves occurring within regularly deposited sediments as they are not influenced by older C sources and are not reworked during flood events. Such samples are rare, however. Therefore, most often, radiocarbon ages tend to be too old because of dating of older, reworked materials. Furthermore, calibration of conventional radiocarbon ages leads to quite large uncertainty ranges between 100 and 500 years, which has to be considered when compiling the age model.

Preparation and pretreatment of sample material for radiocarbon dating were carried out by the ^{14}C laboratory of the Department of Geography at the University of Zurich (GIUZ). The dating itself was done using the accelerator mass spectrometry (AMS) with the tandem accelerator of the Institute of Particle Physics at the Swiss Federal Institute of Technology Zurich (ETH). Radiocarbon ages were calibrated using the calibration program OxCal v. 3.8 (Bronk Ramsey, 1995, 2001; Stuiver et al., 1998). The results of radiocarbon dating and calibration are summarized in Table 1.

5. Lake sediments

The studied lakes are located in the northern Alps of Central Switzerland and the northern Alpine foreland (Fig. 1B). In this area, several lake basins were formed by glacial erosion. Some of these lakes were subject to previous, mainly paleoclimate investigations, which were used to estimate their suitability for paleoseismic studies (e.g., Baldegger See: Lotter et al., 1997; Soppensee: Hajdas et al., 1993; Zuger See and Zürich See: Kelts, 1978). In Vierwaldstätter See, paleoseismic studies were already carried out by Siegenthaler et al. (1987), Siegenthaler and Sturm (1991), and Schnellmann et al. (2002). Within this study, we focus on the smaller surrounding lakes distributed within an area of about 2000 km^2 in order to characterize the regional impact of historic earthquakes. Ideal sites for paleoseismic investigations are lakes showing a continuous, low sedimentation rate with fine, undisturbed bedding. Bioturbation should be absent, which is generally the case in deeper lakes with anoxic bottom water. Furthermore, the lakes should be within the vicinity of the historical epicenters, implying that they have experienced sufficiently high intensities to show traces of seismic

Table 1
Results of radiocarbon dating of sediment cores in Lungerer See, Seelisberg Seeli and Baldegger See. Calibration after calibration program OxCal v. 3.8 (Bronk Ramsey, 1995, 2001)

Lake	Sample	Depth (cm)	Laboratory code	Conventional radiocarbon age (BP)	2σ range of calibrated radiocarbon age (AD)	$\delta^{13}C$ (‰)	Material
Lungerer See	Lng00-1 2 60	170	UZ-4698	555±50	1300–1440	−22.9	Leaves
	Lng00-1 2 61	171	UZ-4938	230±60	1490–1960	−23.6	Leaves
	Lng00-1 5 97	510	UZ-4940	415±50	1410–1640	−20.8	Leaves
	Lng00-1 6 68	580	UZ-4699	365±45	1440–1640	−23.9	Leaves (?)
	Lng00-1 6 97	610	UZ-4641	510±50	1300–1480	−20.9	Leaves
Seelisberg Seeli	Sel01-3 I	90	UZ-4649	365±50	1440–1640	−17.3	Leaves
	Sel01-5 AII 77	210	UZ-4935	555±55	1300–1450	−22.2	Leaves
	Sel01-5 AIII 90	330	UZ-4809	1545±50	410–630	−25.5	Leaves
Baldegger See	Ba02-7b 46	50	UZ-4905	335±55	1440–1660	−22.9	Leaves
	Ba02-7b 58	70	UZ-4904	300±45	1470–1670	−22.9	Plant remains
	Ba02-4b 79	120	UZ-4902	670±50	1260–1410	−20.3	Leaves
	Ba02-4b 97	155	UZ-4903	785±45	1160–1300	−30.2	Plant remains
	Ba97-3 4 78	265	UZ-4690	1625±55	250–570	−22.3	Leaves (?)

activity. Based on these considerations, four lakes were chosen for detailed sedimentological investigations: Sarner See, Lungerer See, Baldegger See, and Seelisberg Seeli. Lake bathymetry, seismic lines, coring sites, and composite lithology logs, including the age model, are shown for each lake in Figs. 2, 3, 4, and 5.

5.1. Sarner See

Sarner See is located in a NNE–SSW-trending valley within the Alps of Central Switzerland at an altitude of 469 m a.s.l. (Fig. 1B). It reaches a maximum water depth of 52 m and has a surface area of about 6 km^2 (Fig. 2). Sarner See has a large clastic input from several major tributaries. The seismic lines show only poor penetration of the seismic signal likely due to gas within the sediments. Eleven short sediment cores were taken along the long axis of the lake and across the deepest part of the basin. Sedimentation is clastic-controlled, resulting in a large number of grey to brown, sandy to clayey, graded turbidites that are a few millimeter up to 20 cm thick. These turbidites were generated by flood events. They show varying lithologies and thickness distributions throughout the lake basin, so that they can be related to different inflows. Regularly deposited sediments consist of millimeter-scale layered light and dark grey silty clays. These alternations probably reflect the seasonally changing input of fluvial sediment load. The sediments were dated using historical flood events and ^{137}Cs activity. Sedimentation rates are rather high, with about 10 mm/year resulting in cores that cover approximately only the last 100 years.

5.2. Lungerer See

Lungerer See lies South of Sarner See, within the same Alpine valley, at an altitude of 689 m a.s.l. (Fig. 1B). The maximum water depth reaches 68 m in the central basin (Fig. 3). The surface area is about 3 km^2. There are several inflows including a major tributary at the southern end. A dense grid of seismic profiles, with good penetration of the seismic signal, was

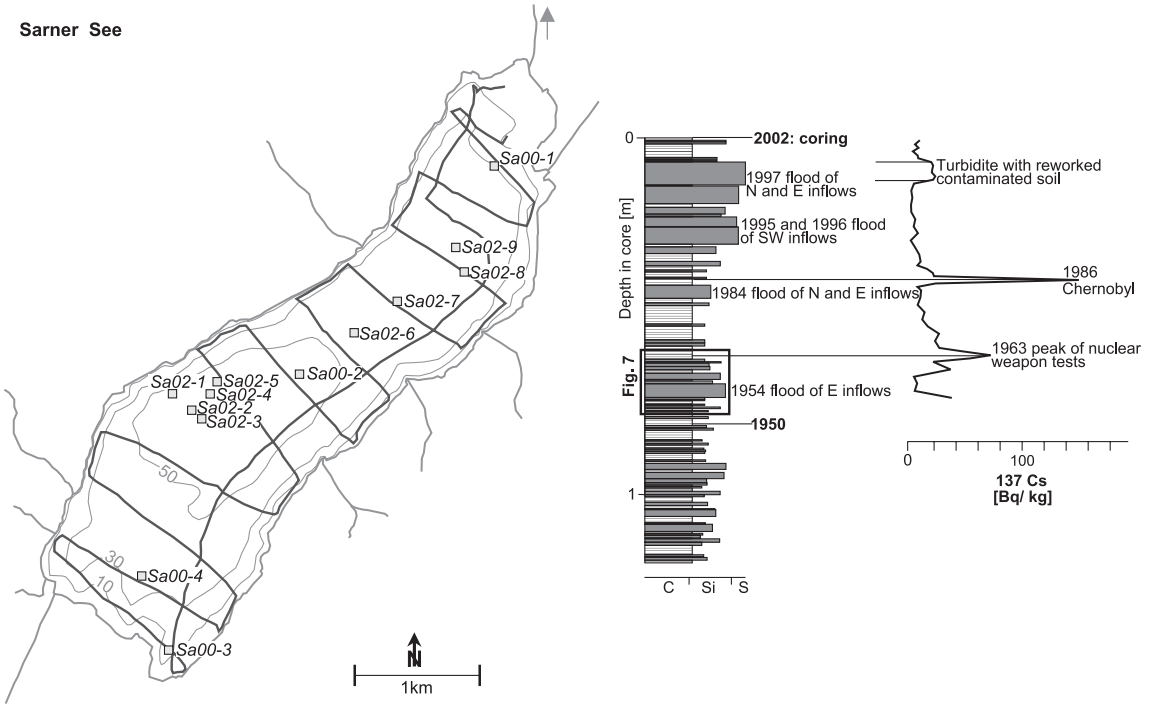

Fig. 2. Seismic survey grid and coring locations in Sarner See with composite lithology log and age control of sediments. Flood events after land register from the Office of Forest and Environment, Kanton Obwalden. All ages are calendar ages AD (legend in Fig. 5).

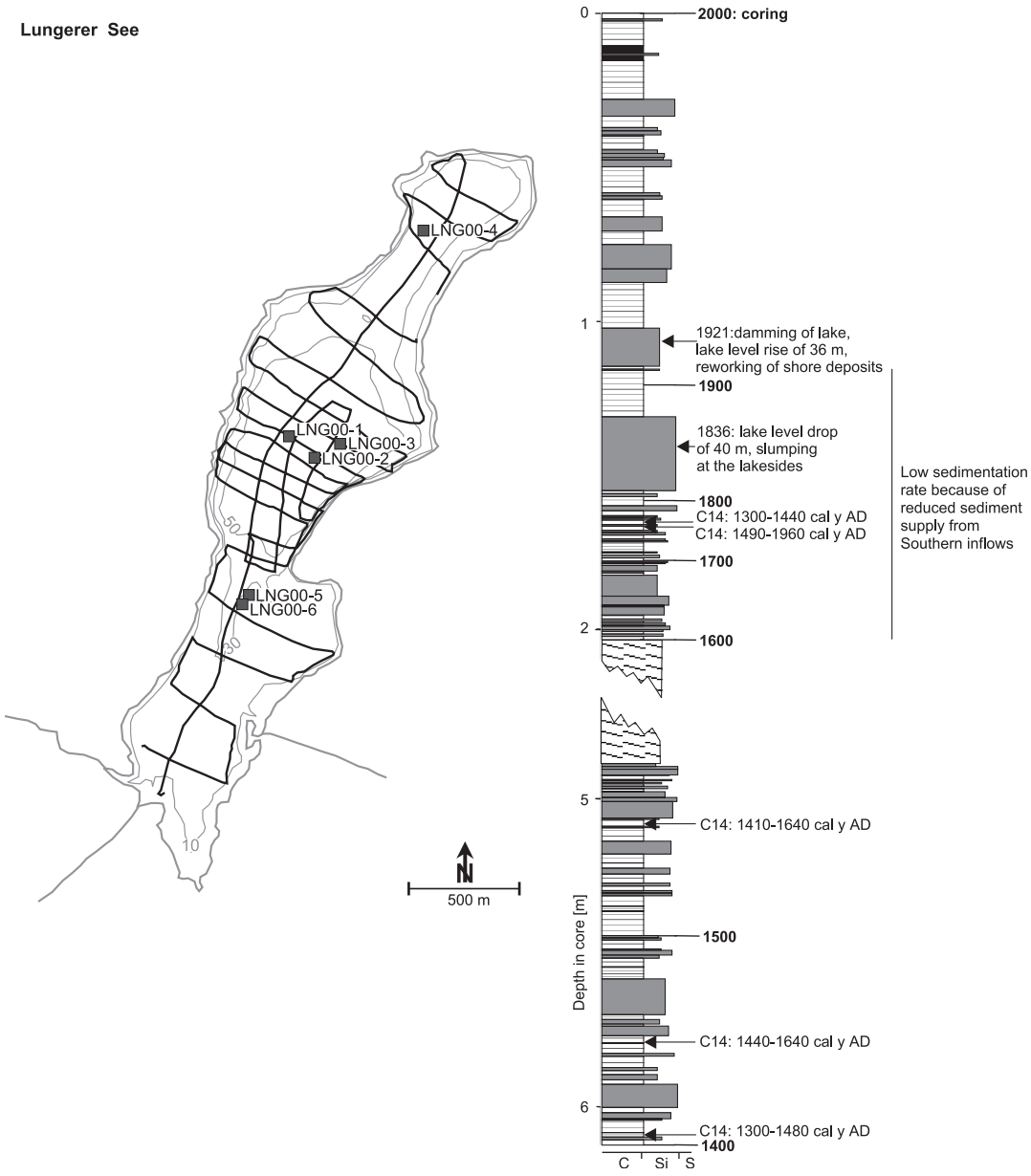

Fig. 3. Seismic survey grid and coring locations in Lungerer See with composite lithology log and age control of sediments in the central basin. Radiocarbon ages are marked as calibrated 2σ age ranges (see Table 1). All ages are calendar ages AD. Lake-level variations after Ming (1991) (legend in Fig. 5).

measured (see description below). Six long sediment cores were collected. Regularly deposited sediment consists of diffusely layered light to dark grey, silty clays that reflect seasonally changing fluvial input. Several sandy to clayey, graded turbidites that range in thickness from a few millimeters up to 20 cm interrupt the normal sedimentation. Furthermore, several-meters-thick lithological units, with largely destroyed bedding, are observed. These are interpreted as slump deposits. Within the younger sedi-

ments, changes in the sedimentary record can be attributed to anthropogenic lake level regulations due to agricultural and hydroelectric use in the area of Lungerer See. Five radiocarbon dates were measured in the older sediments (Fig. 3, Table 1). Sedimentation rates calculated without large slump deposits vary between 2 and 15 mm/year. Sediment cores in the central basin extend to roughly 1400 AD.

5.3. Baldegger See

Baldegger See is located in the northern Alpine foreland at an altitude of 463 m a.s.l. (Fig. 1B). It has a maximum water depth of 68 m and a surface area of 5.2 km^2 (Fig. 4). There are several small tributaries feeding the lake, including a major one at the southern end. The seismic lines show only locally a good penetration of the seismic signal likely due to gas in the sediments. Seven short and six long sediment cores were taken in the deepest part of the basin. The sediments consist mainly of light-brown, carbonate-rich, and organic-rich mud formed by biochemical processes within the lake. They show a weak to well-developed layering. Dark-colored intervals, with a fine lamination at millimeter scale, occur at the top and partly within deeper parts of the core.

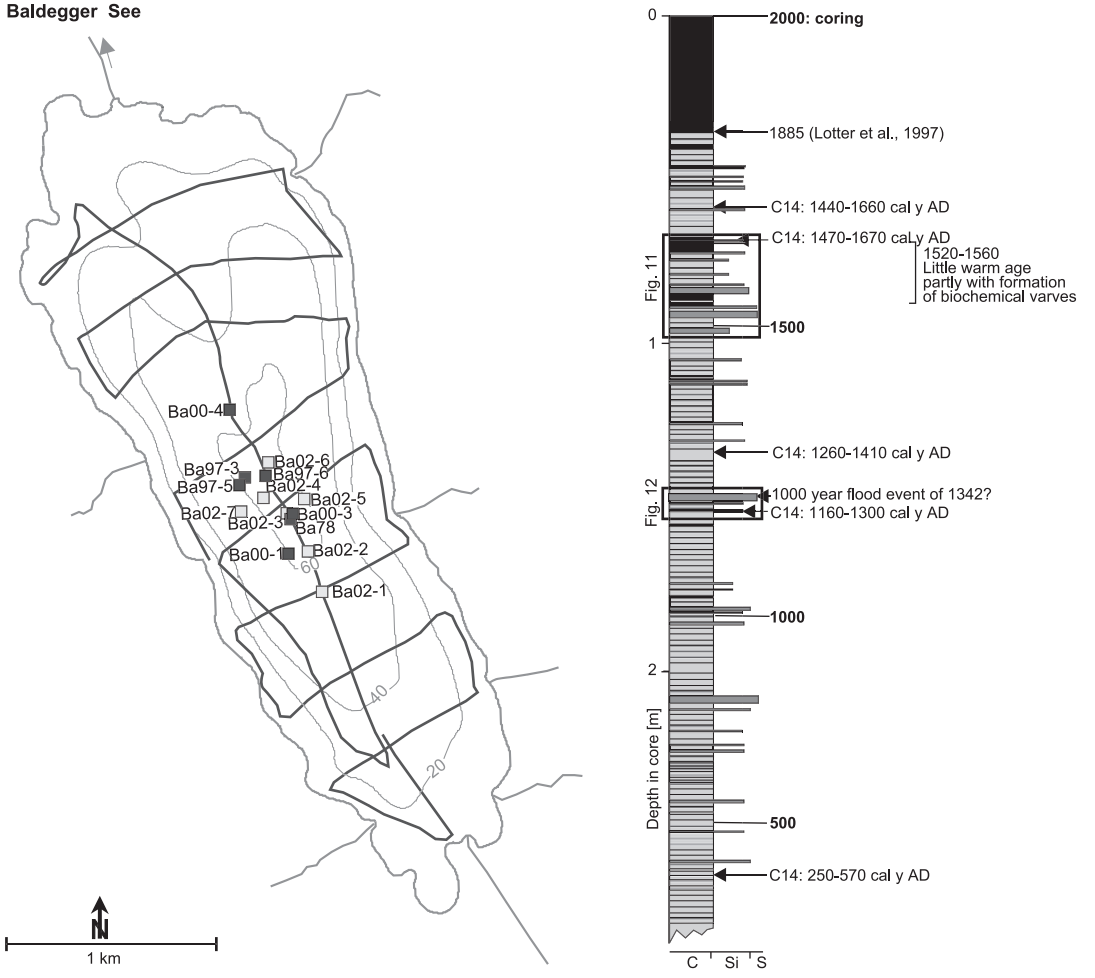

Fig. 4. Seismic survey grid and coring locations in Baldegger See with composite lithology log and age control of sediments. Radiocarbon ages are marked as calibrated 2σ age ranges (see Table 1). All ages are calendar ages AD. Climate data after Pfister (1999) and Pfister and Hächler (1991) (legend in Fig. 5).

They are interpreted as annually deposited, biochemical varves (Lotter et al., 1997). Turbidites or clastic layers generated during flood events are rare and reach only a few centimeters in thickness. The sediments were dated using historical climate data (Pfister, 1999; Pfister and Hächler, 1991) and radiocarbon ages (Fig. 4, Table 1). The long sediment cores cover the entire Holocene and date back to about 13,000 years BC. During the last 1500 years, sedimentation rates are about 1–1.5 mm/year.

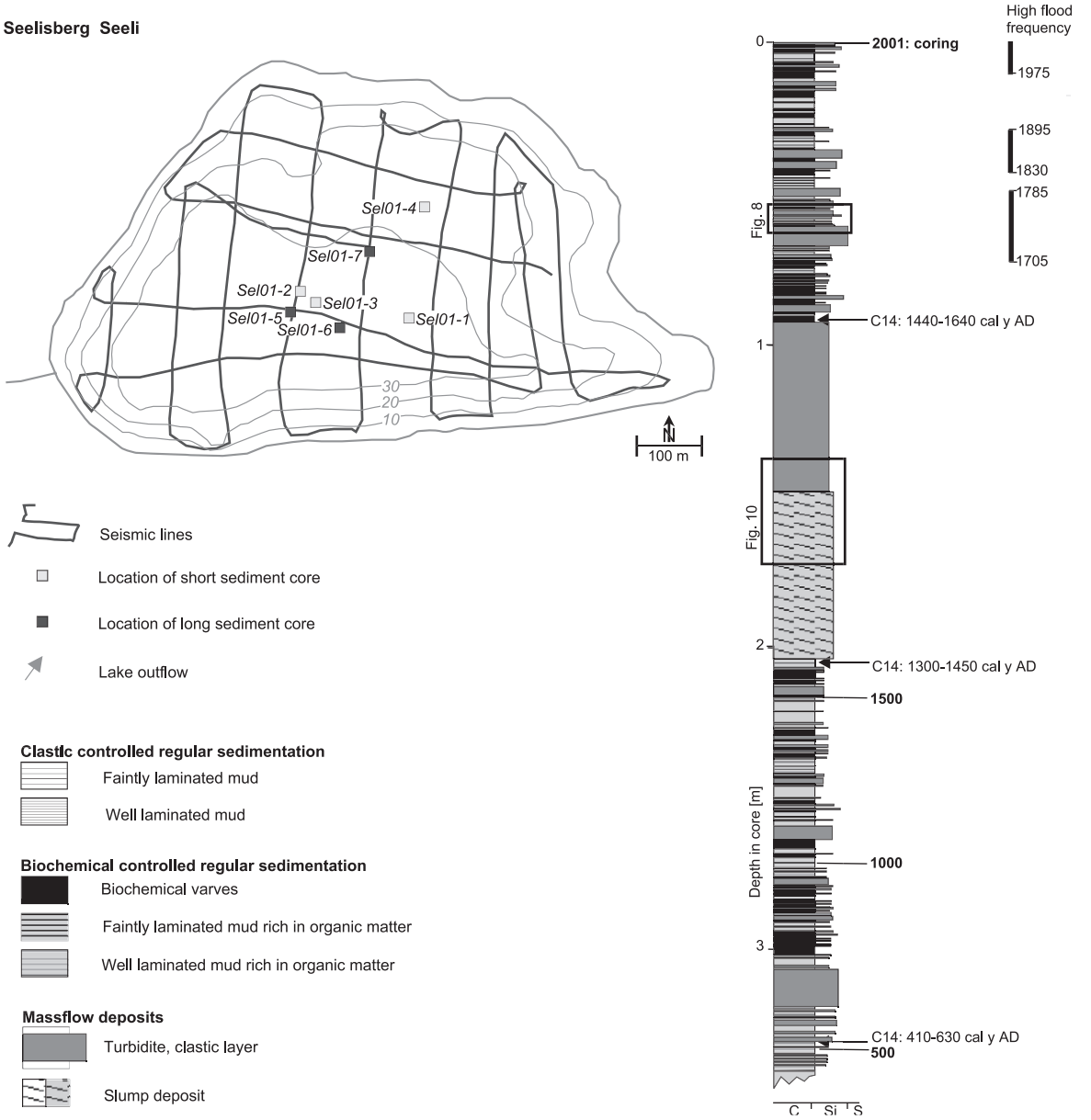

Fig. 5. Seismic survey grid and coring locations in Seelisberg Seeli. Composite lithology log and age control of sediments in Seelisberg Seeli. Radiocarbon ages are marked as calibrated 2σ age ranges (see Table 1). All ages are calendar ages AD. Climate data after Pfister (1999).

5.4. Seelisberg Seeli

Seelisberg Seeli is a small lake located in the Alps of Central Switzerland at 738 m a.s.l. (Fig. 1B). It is formed by karst processes and has a surface area of only about 0.2 km^2 but a maximum water depth of 37 m (Fig. 5). It has one small tributary that is active only during periods of strong rainfalls (Theiler et al., 2003). The seismic profiles show poor penetration of the acoustic signal presumably because of gas in the sediments.

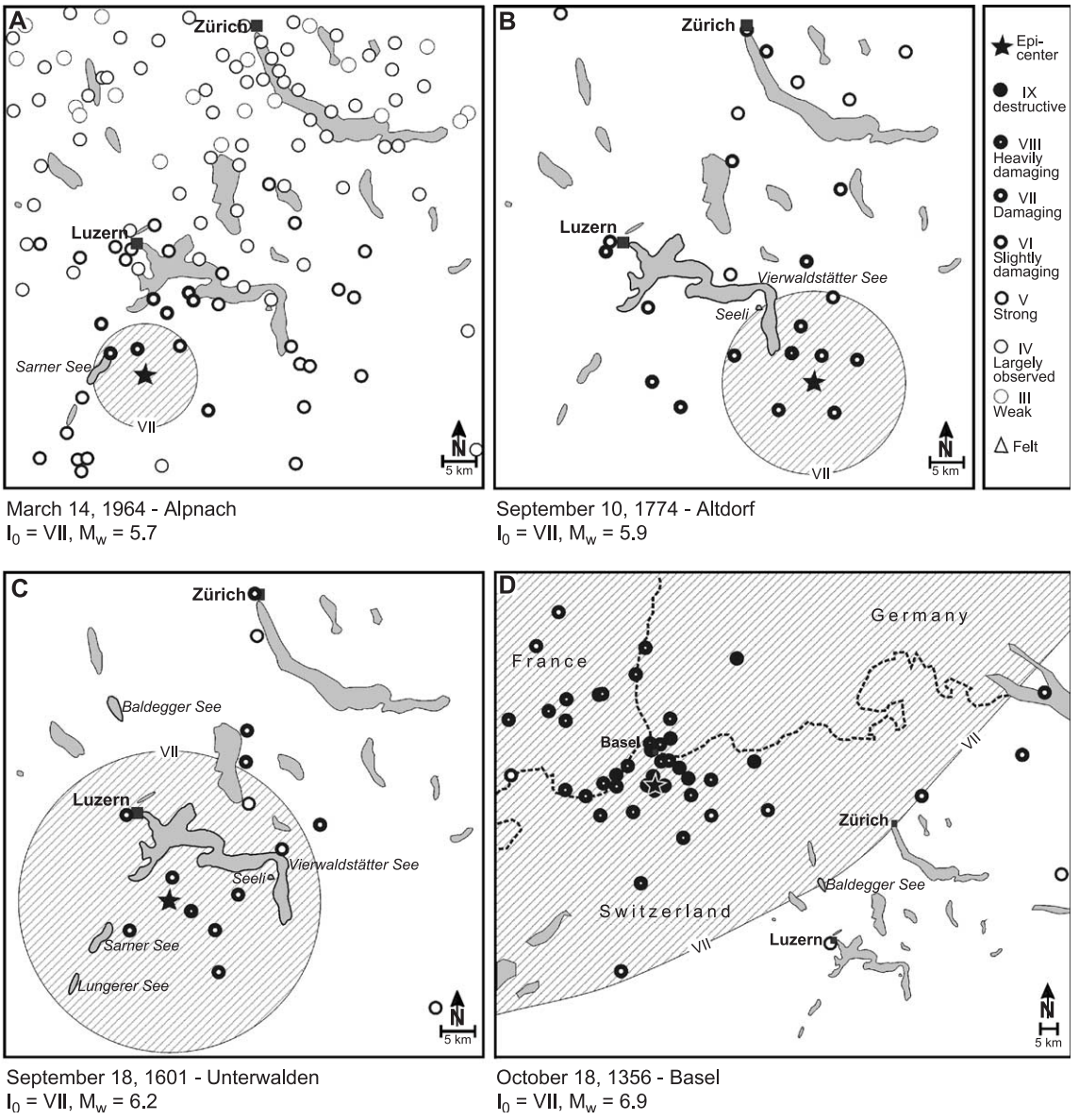

Fig. 6. Macroseismic maps of the four largest historic earthquakes affecting the area of Central Switzerland during the last 1000 years (intensity points from Fäh et al., 2003). Shaded areas mark regions with expected intensity VII and more (intensity attenuation relation for 1964 Alpnach, 1774 Altdorf, and 1601 Unterwalden earthquakes after Swiss Seismological Survey, 2002; 1356 Basel earthquake after Mayer-Rosa and Cadiot, 1979). (A) Macroseismic map of 1964 Alpnach earthquake. (B) Macroseismic map of 1774 Altdorf earthquake. (C) Macroseismic map of 1601 Unterwalden earthquake. (D) Macroseismic map of 1356 Basel earthquake.

Four short and three long sediment cores were taken from the deepest part of the lake. Regularly deposited sediment consists of dark-brown to black, organic-rich, and carbonate-rich mud with abundant plant remains. It often shows a well-developed layering with intervals of annual lamination (biochemical varves). Remarkable is the large number of turbidites or clastic layers, which range in thickness from a few millimeters up to 20 cm and were generated during flood events (Theiler et al., 2003). Units with largely destroyed bedding, which are up to half a meter thick, occur rarely and are interpreted as slump deposits. They are overlain by thick, slump-generated turbidites. The age model is obtained by using historical flood events and radiocarbon ages. The long sediment cores extend to approximately 10,000 years BC. Sedimentation rates in the uppermost part are similar to those of Baldegger See with 1–2 mm/year.

6. Signature of historic earthquakes

Four large earthquakes, with magnitudes of M_w=5.7 to M_w=6.9 and epicentral intensities of I_0=VII to I_0=IX, affected the area of Central Switzerland during the last 1000 years. In Sections 7–10, we describe the lake sediments and deformation structures that can be attributed to these earthquakes.

7. March 14, 1964—Alpnach

On March 14, 1964, an earthquake with M_w=5.7 and I_0=VII occurred about 5 km east of Sarner See (8.32°E/46.87°N) (Fäh et al., 2003; Fig. 6A). It was part of a series of earthquake events occurring over several months with a major event of magnitude M_w=5 occurring only one month before. The earthquake was felt in large parts of Switzerland as well as in southwestern Germany, southeastern France, and northern Italy (Neue Zürcher Zeitung (NZZ), 16.03.1964). Numerous buildings within a radius of 8 km from the epicenter showed substantial damage. The hypocenter was located at a depth of 5–7 km. A focal mechanism proposed by Ahorner et al. (1972) suggests a NNE–SSW-trending, steeply dipping, strike–slip fault. Review of these data, however, revealed no clear solution of the focal mechanism (Deichmann et al., 2000).

7.1. Traces in Sarner See

Because of its proximity to the epicenter, several short sediment cores were taken from the Sarner See to find traces of the 1964 earthquake in the lake sediments. Based on the ^{137}Cs activity profile, the year 1964 AD can be exactly determined in the sedimentary record of Sarner See right above the ^{137}Cs peak of 1963 AD (Figs. 2 and 7). Possible deformation of the lake sediments, during the 1964 Alpnach earthquake, likely disturbed the sediments immediately below the 1964 horizon as deformation of water-saturated sediments is reported to occur close to the water/sediment interface (e.g., Sims, 1973; Sims, 1975; Obermeier, 1996). At greater core depth with increasing compaction and decreasing water content, the liquefaction potential of the sedimentary

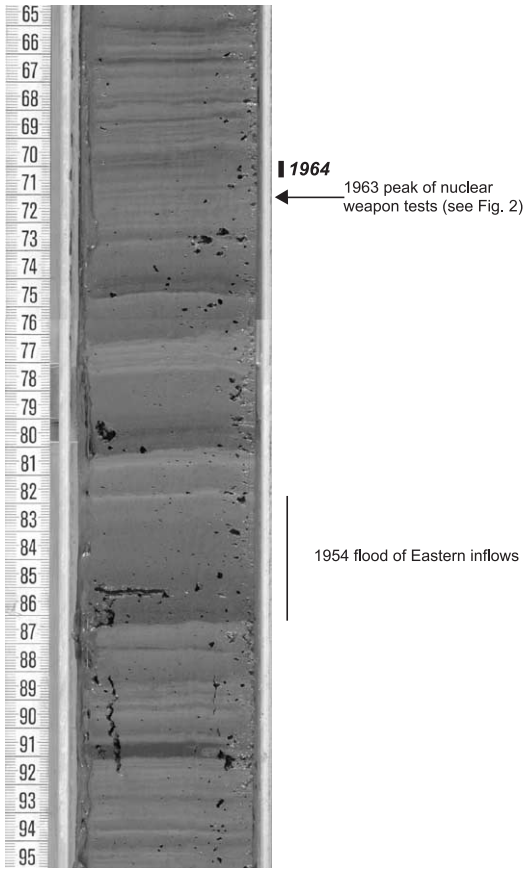

Fig. 7. Undisturbed sediments in Sarner See deposited in the time span of the 1964 Alpnach earthquake.

succession decreases rapidly. The sediments below the 1964 horizon consist of well-laminated, silty clays interrupted by up to 4-cm-thick graded turbidites. In some cores, this succession shows slight disturbances and thickness variations. These features are attributed to primary irregularities in the normal sedimentation. No clear secondary deformation structures, which could have been generated during earthquake ground-shaking, are observed. The clay content probably provides cohesion to the sediments, which may hinder liquefaction or other soft sediment deformations. Therefore, traces of the 1964 Alpnach earthquake could not be found in the sedimentary record of Sarner See.

8. September 10, 1774—Altdorf

The second largest historically reported earthquake in Central Switzerland occurred on September 10, 1774 southeast of Vierwaldstättersee (8.67°E/46.85°N) with a magnitude of M_w=5.9 and an epicentral intensity of I_0=VII (Fäh et al., 2003; Fig. 6B). The maximum intensity close to the epicenter reached I_x=VIII. Major damages corresponding to an intensity of I=VII to I=VIII were reported within a radius of about 14 km from the epicenter. Historical sources report several landslides and rockfalls (e.g., a piece of land was sliding into the southeastern basin of Vierwaldstättersee) (Deichmann et al., 2000; Heer, 1975). Water in the fountains became turbid and two people were killed by falling chimneys and rocks.

In a previous study in the southeastern basin of Vierwaldstättersee, rockfall and slump deposits were correlated to the 1774 earthquake (Siegenthaler and Sturm, 1991). However, in the sedimentary record of the northwestern part of Vierwaldstättersee, there is no evidence of any deformation corresponding to this earthquake (Schnellmann et al., 2002).

8.1. Traces in Seelisberg Seeli

In the present study, only very small but significant deformation structures were found in three of seven cores from Seelisberg Seeli, which is situated at 10 km distance from the historical epicenter. At a depth of 60 cm within carbonate-rich finely laminated sediments, a 2-cm-long normal fault with a displacement of 1–2 mm occurs (Fig. 8). Furthermore, slight deformations such as disrupted layers and incipient liquefaction within turbiditic silts were observed within the same stratigraphic level. Earthquake-induced faulting has been reported by several authors, but often at a larger scale and sometimes linked with clear liquefaction structures (e.g., Seilacher, 1969; Ringrose, 1989; Becker et al., 2002). As carbonate mud starts to lithify early, these sediments quickly gain enough strength so that brittle failure may occur. The observed deformations are similar to the lowest deformation level described by Ringrose (1989) for a paleoseismic event in Scotland with fissuring and slight deformations at the centimeter scale. Such deformations are not continuous within one stratigraphic horizon but are separated by undisturbed zones. This explains that in Seelisberg Seeli, only a few cores show deformation structures, whereas other cores are completely undisturbed. Normal faulting could have also been caused by sediment overloading and compaction; however, there is no evidence of rapid and large sediment loading. Furthermore, creep of sediments is unlikely to be observed in these cores as they were taken in the deepest, flat-lying part of the basin.

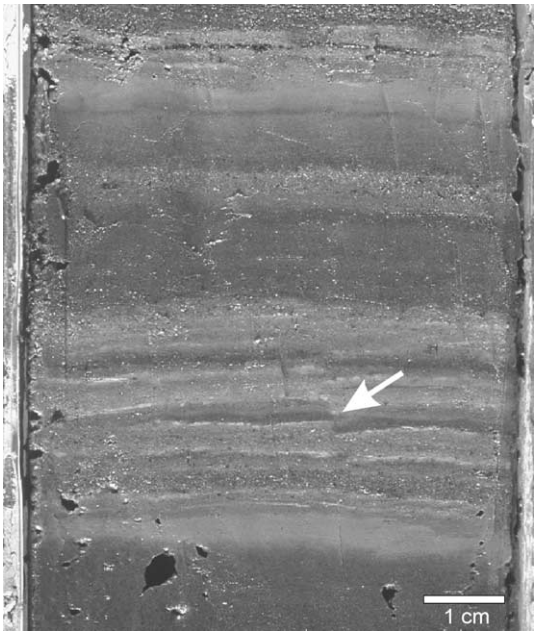

Fig. 8. Microfault attributed to the 1774 Altdorf earthquake within finely laminated sediments from Seelisberg Seeli (sediment core Sel01-3; 60 cm).

8.1.1. Dating of deformation

At roughly 1 m core depth, a slump deposit including a thick slump-generated turbidite occurs (Fig. 5). These deposits correlate with the 1601 Unterwalden earthquake (see description below). The overlying 1-m-thick succession thus should correspond to the time span between the 1601 earthquake and the coring in 2001. Varve counting is possible only in some intervals, but it matches well with the average sedimentation rate of about 1.5–2 mm and places the year 1774 AD right above the deformed horizon. Furthermore, periods of high flood frequency compiled by Pfister (1999) from historical data can be related to intervals with an increased number of turbidites. The year 1774 AD would be at the top of a period of high flood frequency from 1705 AD to 1785 AD right above the deformed horizon.

9. September 18, 1601—Unterwalden

On September 18, 1601, an earthquake occurred south of Vierwaldstättersee (8.36°E/46.92°N) with a magnitude of M_w=6.2 and an epicentral intensity of I_0=VII (Fäh et al., 2003; Fig. 6C). It is among the strongest events in Switzerland during the last millennium and has become well known because of the detailed description of Renward Cysat, the municipal clerk of Luzern at that time (Papastamatiou, 1983; Schwarz-Zanetti et al., 2003). Cysat (1601) reports major to heavy damages (intensities between VII and VIII) within a radius of at least 23 km from the epicenter. Several masonry buildings and most of the stoves close to the epicenter were entirely destroyed. Some towers and churches had to be pulled down and rebuilt. Luzern was severely hit by the earthquake as chimneys and tiles fell and walls cracked in part of the city. Remarkable are large water movements in Vierwaldstättersee: a 1- to 2-m-high standing wave (seiche) oscillated in the lake for several days. This observation led to intensive investigations in Vierwaldstättersee that revealed numerous large slump deposits, which were generated during the earthquake (Siegenthaler et al., 1987; Siegenthaler and Sturm, 1991; Schnellmann et al., 2002). Because of the high intensity and the epicenter in the middle of the study area, we expected to find traces of the 1601 earthquake in the lakes surrounding Vierwaldstätter See.

9.1. Traces in Lungerer See

In Lungerer See, at about 20 km distance to the historical epicenter, the seismic lines image a wide (up

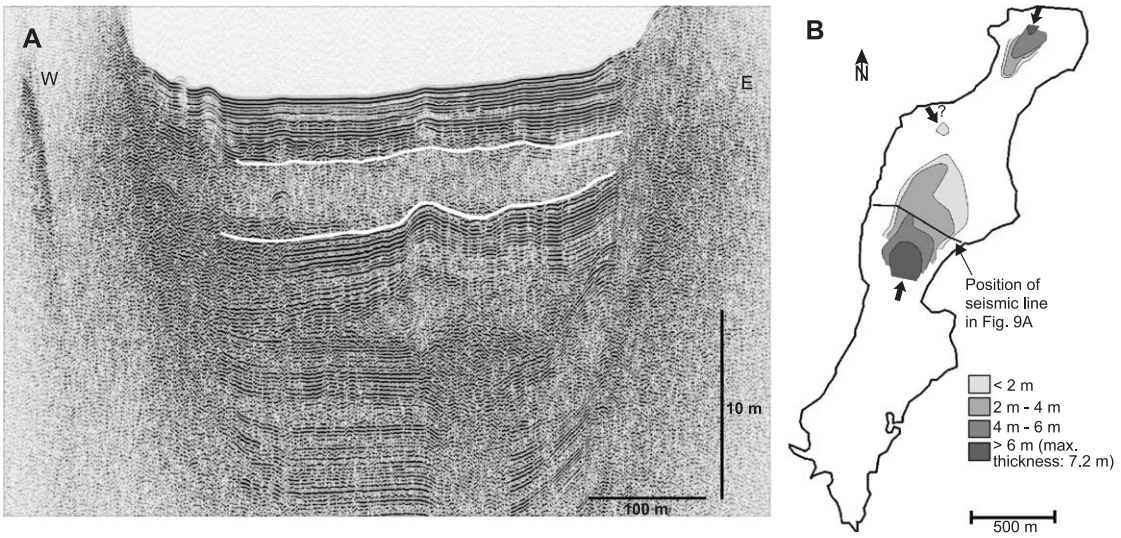

Fig. 9. (A) Seismic line through central basin of Lungerer See. Horizontally layered seismic facies represents regular sedimentation. Chaotic seismic facies indicates slump deposit. White lines mark slump deposit related to the 1601 Unterwalden earthquake. (B) Thickness distribution of the 1601 slump deposit in the northern and central basins of Lungerer See.

to 7.2 m thick) unit of chaotic seismic facies with the top at a depth of about 2 m (Fig. 9A). Cores from the central basin of Lungerer See pass through this unit and show structureless silty clays with intraclasts of gravels, wood, and soil. Also larger sections of nearly undisturbed lake sediments are incorporated within the massive clays. The thickness distribution of this unit indicates three different depositional centers (Fig. 9B). The unit is interpreted as multiple slump deposit produced by simultaneous slumping at different lake sides. The largest slump unit in the central basin was generated within delta deposits in the southern basin. Multiple slumping implies a regional triggering mechanism such as an earthquake.

9.1.1. Dating of deformation

Three radiocarbon ages were obtained below the slump deposit (Fig. 3). The resulting depth/age relationship in the lower sediments gives an average sedimentation rate of 0.56 cm/year, which would place the year 1601 AD right below the slump deposit. On top of the slump deposit, major turbidites and changes in sedimentation can be attributed to anthropogenic lake level regulations in the 19th and early 20th centuries. According to two radiocarbon ages, the sedimentation rate above the slump deposit could be estimated at 0.24 cm/year. Extrapolating this relation to the top of the slump deposit, the timing of slumping is in the range of the 1601 earthquake. The highly reduced sedimentation rate from 1601 AD to 1921 AD can be explained by reduced sediment supply from the southern basin, as part of the southern delta collapsed during slumping. Furthermore, from 1836 AD to 1921 AD, the whole southern sediment supply was cut off because of the artificial lake level low stand. In 1921 AD, the lake was dammed again. From that time, annual lake level oscillations (up to 40 m) caused by a hydroelectric power station led to an enhanced reworking of shore deposits and thus highly increased sedimentation rates.

9.2. Traces in Seelisberg Seeli

The cores of Seelisberg Seeli in a depth of 1.50 m contain a 40- to 60-cm-thick unit with overturned and completely destroyed bedding and several fragments of cretaceous limestone (Figs. 5 and 10). It is overlain by a 20- to 60-cm-thick, graded, sandy to clayey

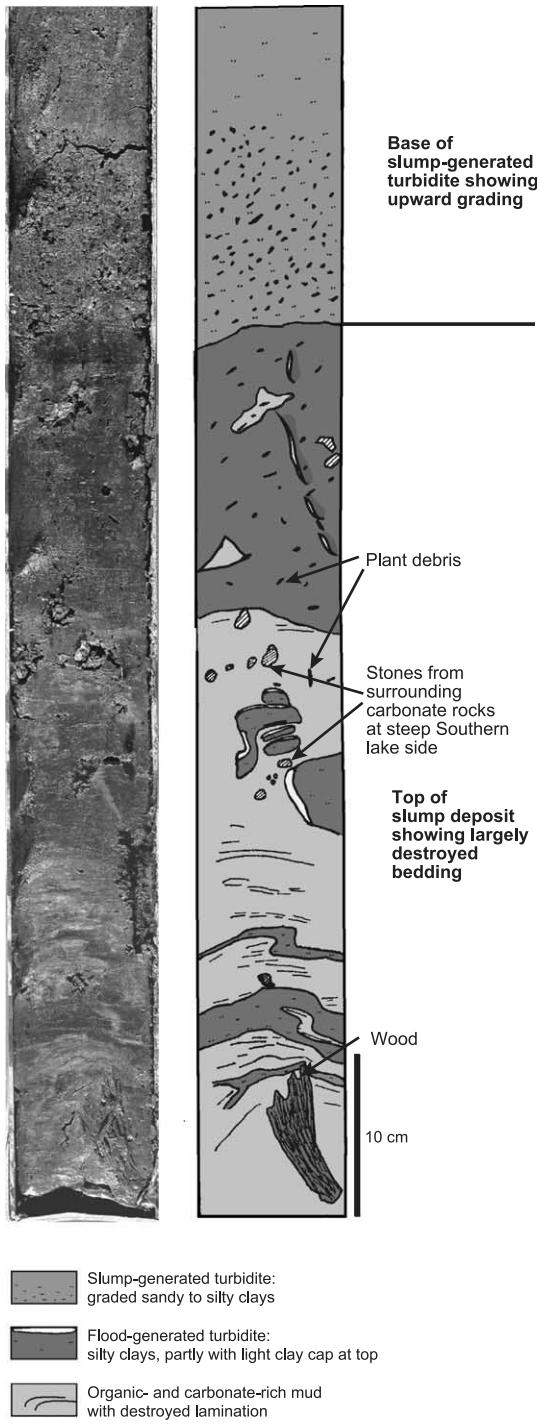

Fig. 10. Slump deposit related to the 1601 Unterwalden earthquake in sediments of Seelisberg Seeli (sediment core Sel01-6A; 110–180 cm). The figure shows the uppermost part of the slump deposit with largely destroyed bedding and the overlying slump-generated turbidite.

turbidite. These deposits were generated by slumping at the lake sides combined with, or probably triggered by, a rockfall at the steep southern lakeside of Seelisberg Seeli. A lot of material was brought into suspension during slumping, leading to the deposition of a thick turbidite that covers the slump deposit ("homogenite" after Siegenthaler et al., 1987).

9.2.1. Dating of deformation

The sediments above the slump deposit can be dated by varve counting and correlation of periods of high flood frequency after Pfister (1999) (Fig. 5). They correlate well to the timespan between the 1601 earthquake and the coring in 2001 (see dating of 1774 Altdorf earthquake). Furthermore, radiocarbon ages were obtained right below and above the slump deposit. The lower age is likely too old because of erosion during slumping or the dating of reworked material. The upper age fits quite well with the 1601 earthquake so that, most probably, the slump in Seelisberg Seeli was generated during this earthquake.

9.3. Traces in Baldegger See

In contrast to these large-scale slump deposits, much smaller in situ deformation structures were observed in Baldegger See, which is at 30 km distance to the epicenter. In 6 of 10 cores, at a core depth of about 60 cm, clear deformation structures occur within a zone up to 40 cm thick. They include microfaults, folds, disrupted layers, and loading structures with carbonate-rich sediment sunk into turbiditic silts (Fig. 11). These small-scale features are interpreted as earthquake-induced in situ deformations similar to those described by Rodriguez Pascua et al. (2000) and Marco et al. (1996) for well-laminated lake sediments. Carbonate mud has a high initial lithification rate and reaches a considerable strength and density shortly after deposition (Weaver and Jeffcoat, 1978). Therefore, it may show brittle failure during earthquake shaking, leading to small microfaults and disrupted layers. Furthermore, it is denser than turbiditic silts. The latter were liquefied during the earthquake, so that overlying heavier carbonate mud sank into the turbidite material (cf. Anketell et al., 1970). Microfolds are the result of shear stress applied to poorly lithified sediment for instance during earthquake shaking.

9.3.1. Dating of deformation

The deformational event must have taken place shortly after deposition because of the higher potential of soft sediment deformation close to the water/sediment interface (Sims, 1973; Sims, 1975; Obermeier, 1996). The cores of Baldeggersee are very well dated (Fig. 4). Varve counting is possible in

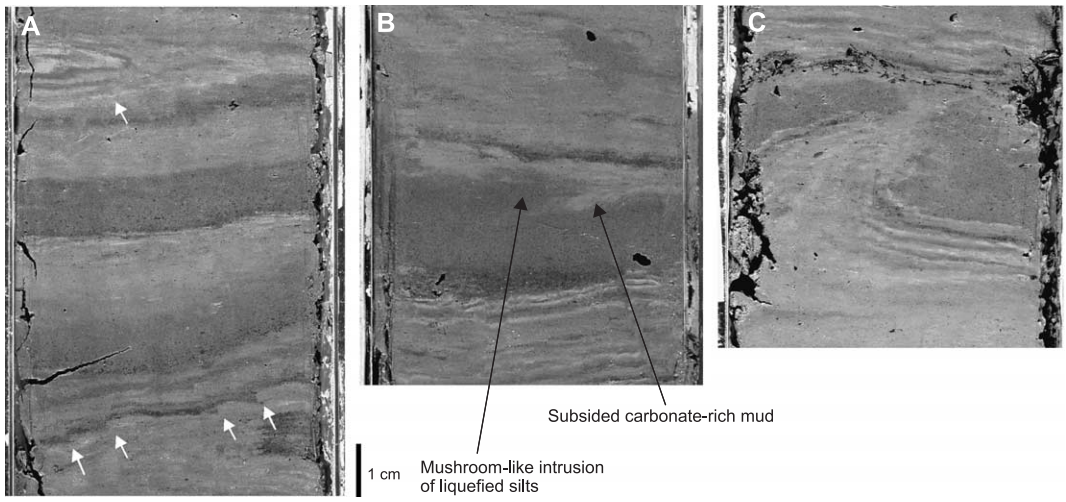

Fig. 11. Deformation structures observed in different sediment cores from Baldegger See and related to the 1601 Unterwalden earthquake. (A) Microfolds and microfaults (marked with arrows) (sediment core Ba02-4; 80–90 cm). (B) Liquefaction structure: carbonate-rich mud sunk into liquefied turbiditic silts (sediment core Ba97-3; 85–90 cm). (C) Folded and disrupted layers (sediment core Ba02-7; 80–85 cm).

the uppermost 30 cm back to the year 1885 AD (Lotter et al., 1997). The observed deformation structures occur in a depth of about 60–90 cm also in zones with biochemical varves. These varves form under nutrient-rich conditions and are likely related to the so-called Little Warm Age lasting from 1520 AD to 1560 AD (Pfister, 1999). Deformation of these varved units must have taken place shortly after their deposition, which corresponds well with the 1601 earthquake. Furthermore, five radiocarbon ages were measured within the uppermost 3 m, allowing a good depth/age relationship. Two radiocarbon ages that are only slightly older than 1601 AD were obtained right above the deformed horizon.

10. October 18, 1356—Basel/BS

On October 18, 1356, the city of Basel was hit by the strongest historically known earthquake in Mid Europe, north of the Alps (7.6°E/47.47°N; Fäh et al., 2003; Mayer-Rosa and Cadiot, 1979). It had a moment magnitude of M_w=6.9 and an epicentral intensity of I_0=IX (Fig. 6D). Within a radius of about 30 km, nearly all churches and castles were destroyed. Major damages corresponding to intensity VII occurred in an area of 60 000 km^2. The "red book of Basel" reports (translated into English): "...this town was destroyed and broken by the earthquake and no church, tower, or house of stone in this town or in the suburb endured, most of them were destroyed..." According to different authors, the number of lives lost varies between 100 and 2000. This relatively low number can be explained by a strong foreshock that sent most people into the streets. Paleoseismic studies focused on fault trenching (Meghraoui et al., 2001), damage of stalagmites in caves (Lemeille et al., 1999), and slope instabilities (Becker and Davenport, 2003). First investigations of lake deposits in the Basel area were carried out by Becker et al. (2002). They found several earthquake-induced structures linked to prehistoric earthquakes but no traces of the 1356 earthquake due to unfavourable conditions in lake sedimentation during that time.

10.1. Traces in Baldegger See

Within this study, small-scale deformation structures were observed in two cores of Baldegger See, which is situated at a distance of 57 km from the epicenter. At a depth of 140 cm, a 0.5- to 2-cm-thick, sandy to silty, clastic layer is overlain by carbonate-rich mud (Figs. 4 and 12). In one core, the sand forms a mushroom-like structure protruding into the carbonate mud. In a second core, lenses of carbonate mud are sunk into the clastic material (Fig. 12). Furthermore, slight disturbances in the layering and disrupted layers occur below the clastic layer. These structures are interpreted as earthquake-induced soft sediment deformations with mushroom-like intrusions and pseudonodules as described, for example, by Rodriguez Pascua et al. (2000). The sandy silts were

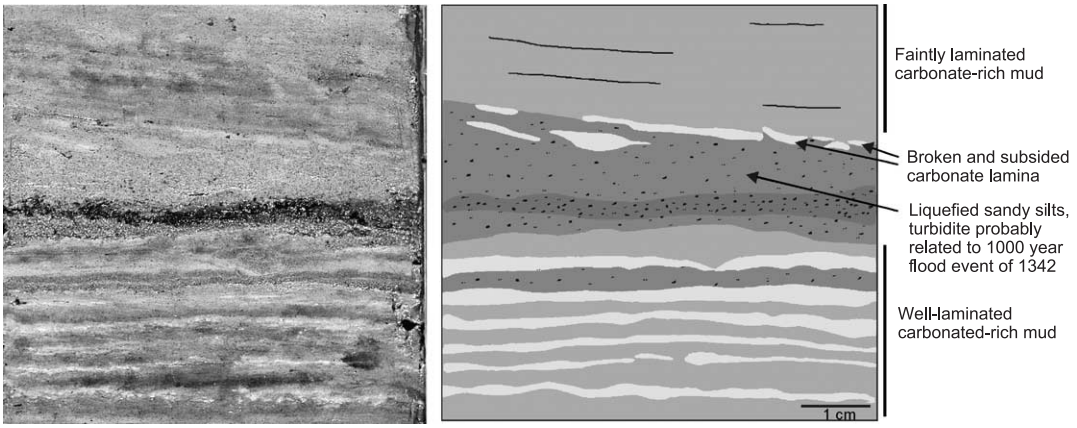

Fig. 12. Liquefaction structure (pseudonodules) related to the 1356 Basel earthquake within sediments of Baldegger See (sediment core Ba00-3; 210–215 cm). Carbonate-rich mud above sandy to silty layer is broken into pieces and sunk into liquefied material.

liquefied during earthquake shaking so that the denser and more cohesive carbonate mud was sinking into the liquefied material while lighter, liquefied material was intruding into the overlying carbonate mud (cf. Anketell et al., 1970). More brittle deformation with disturbed and disrupted layering occurred within the already more lithified part in greater depth below the clastic layer. Hints of other liquefaction-inducing processes like wave action, rapid sediment load, or large lake-level variations are missing in the environmental and sedimentary records of Baldegger See.

10.1.1. Dating of deformation

As liquefaction occurs only in water-saturated sediments, the deformation must have taken place close to the water/sediment interface shortly after deposition of the clastic layer (cf. Sims, 1973; Sims, 1975; Obermeier, 1996). In 1342 AD, a 1000-year flood event occurred in Mid Europe (Pfister and Hächler, 1991) (Figs. 4 and 12). The liquefied layer is one of the thickest, coarse-grained layers within the sedimentary record of Baldegger See during the last 15,000 years. It was probably deposited during this flood event and became deformed by the 1356 Basel earthquake. Furthermore, radiocarbon ages were obtained right below and above the deformed sequence and are only slightly older than 1356 AD (Fig. 4).

11. Discussion

Fig. 13 summarizes the observed deformation structures in relation to the historically reported

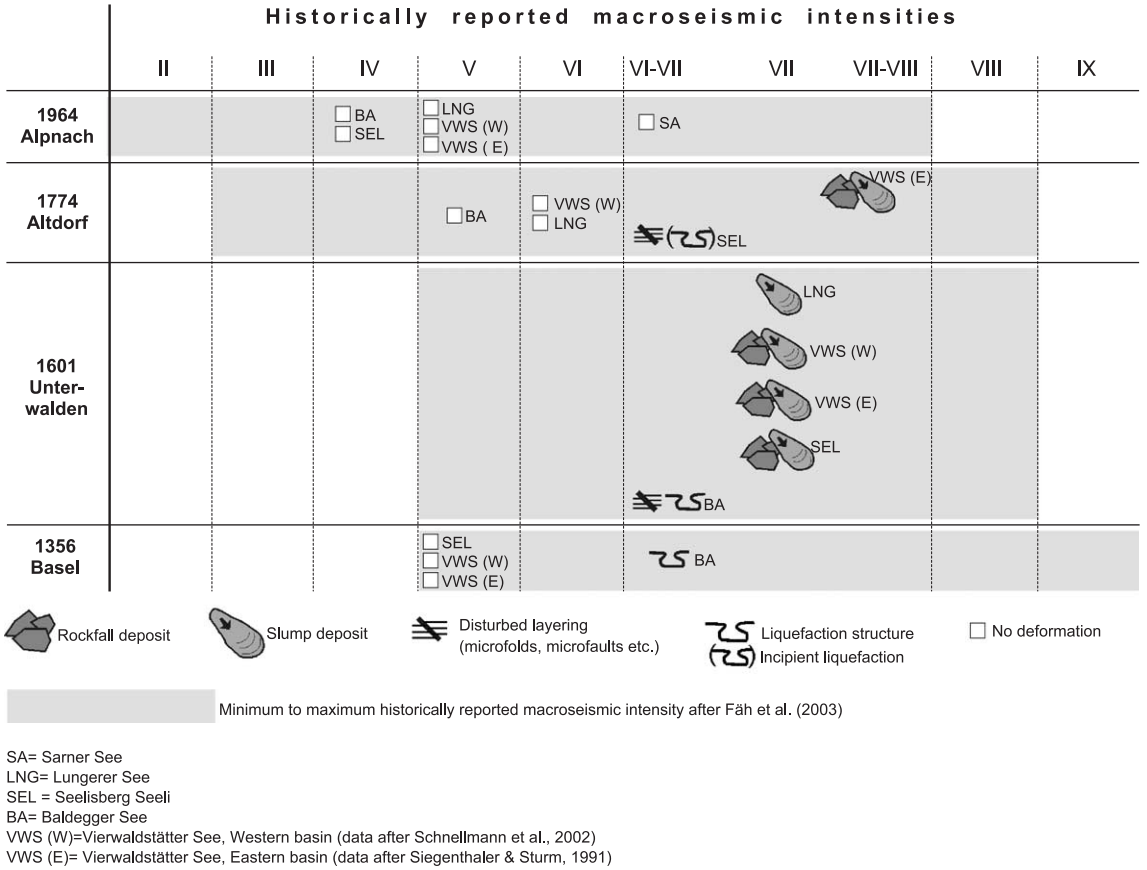

Fig. 13. Correlation of earthquake-induced deformation structures to historically reported macroseismic intensities from Fäh et al. (2003) (see Fig. 6). The dataset shows that the threshold for sediment deformation during earthquake shaking lies at intensities VI to VII.

macroseismic intensities of the four investigated earthquakes. Numerous factors control the type, size, and extent of earthquake-induced deformation structures. This includes seismological factors like the duration of earthquake shaking, shaking amplitude, and frequency. Furthermore, sediment type, geometry of the lake basin, and amplification of shaking due to site effects play an important role. Therefore, deformation features can vary widely within a local area. However, our dataset shows that deformation structures start to be formed during groundshaking of intensity VI to VII (Fig. 13). Small-scale structures,

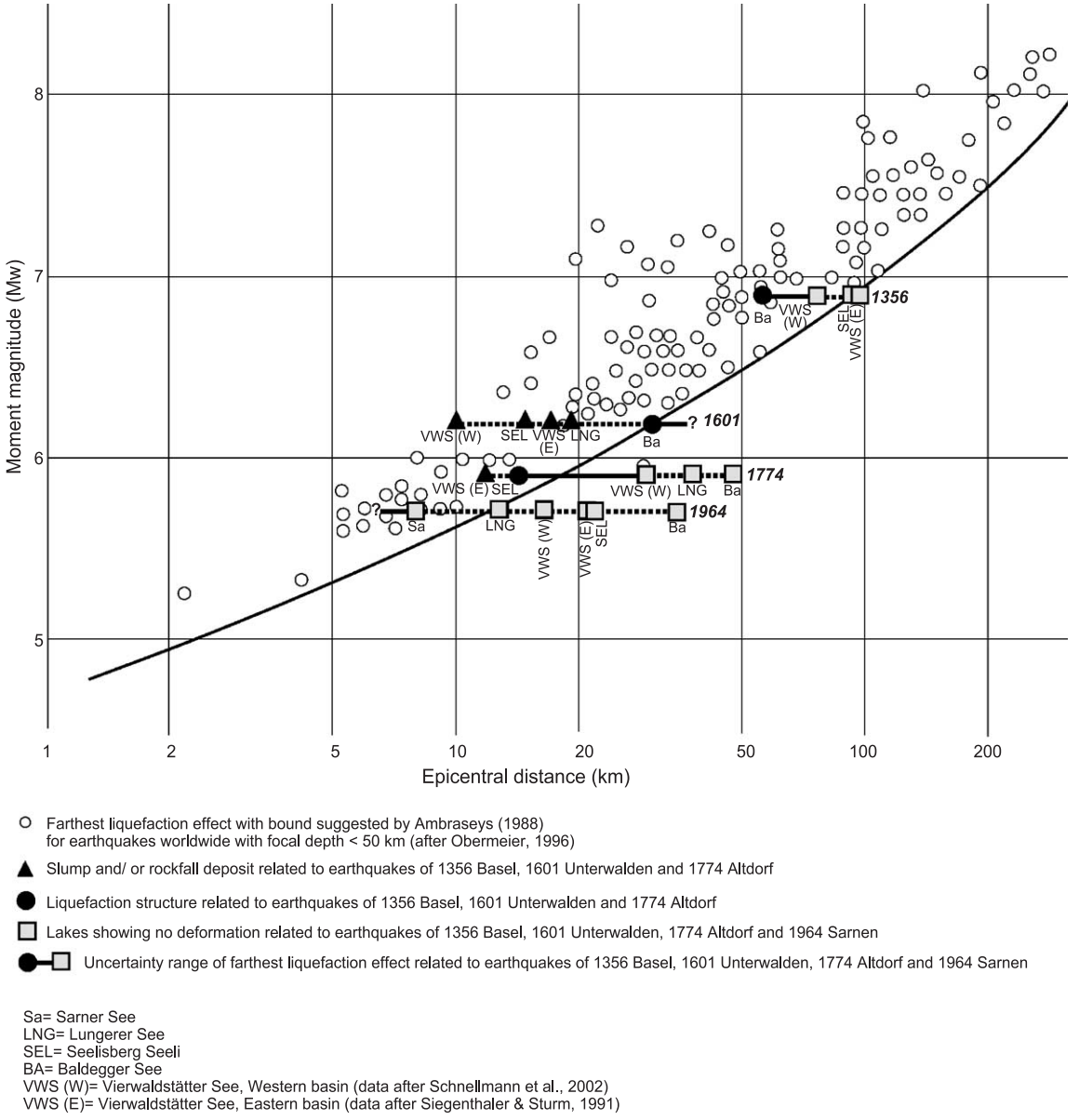

Fig 14. Positive and negative evidence of deformation in lake deposits during historic earthquakes in relation to moment magnitudes (M_w) after Fäh et al. (2003). Open circles: Relationship between earthquake moment magnitude (M_w) and epicentral distance to the farthest liquefaction structure of earthquakes worldwide with bound curve proposed by Ambraseys (1988) (modified after Obermeier, 1996).

like disturbed and contorted lamination as well as liquefaction structures, dominate at lower intensities of VI to VII. Towards higher intensities, large-scale mass movements, like slumps and rockfalls, become more frequent and probably overprint small-scale structures. These observations complement previous studies: Galli and Ferelli (1995) and Obermeier (1996) state that liquefaction structures become common at groundshaking of intensity VII. This is in agreement with experimental data indicating that the threshold for liquefaction lies at magnitude 5–5.5 (Moretti et al., 1999). Paleoseismic investigations in outcrops of lake deposits reveal threshold values of intensity VI for the formation of soft sediment deformation structures (Sims, 1973, 1975; Hibsch et al., 1997). Rodriguez Pascua et al. (2000, 2003) related soft sediment deformation structures within Miocene lake deposits to magnitudes even smaller than 4. However, in core samples and within our types of sediment, no deformation structures related to intensities lower than VI to VII could be found.

In situ soft sediment deformation structures are widely used to determine earthquake size (e.g., Ringrose, 1989, Obermeier, 1996, Rodriguez Pascua et al., 2000, 2003). Obermeier (1996) compiles liquefaction features of numerous earthquakes worldwide in different sedimentary environments and tectonic settings (Fig. 14). The distance from the epicenter to the farthest observed liquefaction structure is related to the reported earthquake magnitude. Liquefaction effects are, for example, venting of sand to the ground surface or ground fissuring mainly within floodplain deposits. The resulting curve provides a minimum estimate of earthquake moment magnitude (magnitude-bound method). In contrast to the dataset of Obermeier (1996), we investigated lake sediments with deformation structures at a much smaller scale. Furthermore, only scattered information about the occurrence and lateral development of soft sediment deformation is available because of the limited extent of lakes. However, using the dataset of Obermeier (1996), we plotted the epicentral distances of lakes with positive and negative evidence of deformation to magnitudes after Fäh et al. (2003) (Fig. 14). The uncertainty range of earthquake size lies between the farthest observed liquefaction structure and the closest lake with no deformation. Our data match very well the dataset of Obermeier (1996) and datapoints are in the range of the uncertainties. No traces of the 1964 Alpnach earthquake were found in the lake sediments. This could be explained by clay-rich sediments, which might have hindered liquefaction and soft sediment deformation. Furthermore, the duration and/or amplitude of shaking probably was not high enough as this M_w=5.7 event is close to the threshold for liquefaction, which is at about magnitude 5–5.5 (Moretti et al., 1999). The relation of the 1774 Altdorf earthquake is somehow uncertain as only very slight deformation structures with incipient liquefaction occur within the sediments of Seelisberg Seeli. This could have been caused by a less intense shaking due to site effects as the lake is situated on hardrocks. Traces of the 1601 Unterwalden earthquake were found in all the investigated lakes. Negative evidence of deformation structures is missing and therefore a minimum magnitude limit cannot be estimated from our data. Considering the clear and widespread deformation features within a zone of up to 40 cm in the sediments of Baldegger See, we suppose that the 1601 earthquake could have been even stronger than calculated from historical data. However, data from more distant lakes are necessary to confirm this. Slight deformation structures related to the 1356 Basel earthquake were found only in Baldegger See. Unfortunately, in this case, there are no data of lakes closer to the epicenter, which would allow a better understanding of the lateral development of deformation.

12. Conclusions

The results of this study show that traces of strong, historic earthquakes are recorded in the sedimentary archive of recent lake deposits using high-resolution seismic data and sediment cores. The occurrence and kind of deformation depend on seismological factors, site effects, and sediment type. The spatial distribution of deformation structures reflects the historical macroseismic dataset. Small-scale soft sediment deformation structures start to form at intensities of VI to VII. Large-scale slumps and rockfalls become more frequent at higher intensities. The small-scale soft sediment deformation structures can be used to estimate minimum values of earthquake size, providing additional data for historical macroseismic data-

sets. Furthermore, this study allows the recognition and calibration of earthquake-induced deformation structures in prehistoric lake sediments and can be used to extend historic earthquake records further back into the Holocene.

Acknowledgements

We thank Miguel Rodriguez Pascua and an anonymous reviewer for helpful comments on a previous version of the manuscript, and Chris Krugh for careful editing. We thank Amik Theiler, Adi Gilli, and Michael Schnellmann for their help during field and laboratory work; and Robert Hofmann, Urs Gerber, Alois Zwysig, and Richard Niederreiter for technical support. This study is part of the Paleoseis Project that is funded by the Swiss National Funds (SNF) and the Swiss Commission for the Safety of Nuclear Installations (HSK).

References

Ahorner, L., Murawski, H., Schneider, G., 1972. Seismotektonische Traverse von der Nordsee bis zum Apennin. Geol. Rundsch. 61, 915–942.

Ambraseys, N.N., 1988. Engineering seismology. Earthquake Eng. Struct. Dyn. 17, 1–105.

Anketell, J.M., Cegla, J., Dzulynski, S., 1970. On the deformational structures in systems with reversed density gradients. Ann. Soc. Geol. Pol. XL, 3–30.

Becker, A., Davenport, C.A., 2003. Rockfalls triggered by the AD 1356 Basle Earthquake. Terra Nova 15 (4), 258–264.

Becker, A., Davenport, C.A., Giardini, D., 2002. Paleoseismicity studies on end-Pleistocene and Holocene lake deposits around Basle, Switzerland. Geophys. J. Int. 149, 659–678.

Bonjer, K.-P., 1997. Seismicity pattern and style of seismic faulting at the eastern borderfault of the Southern Rhine Graben. Tectonophysics 275, 41–69.

Bronk Ramsey, C., 1995. Radiocarbon calibration and analysis of stratigraphy: the OxCal Program. Radiocarbon 37 (2), 425–430.

Bronk Ramsey, C., 2001. Development of the radiocarbon program OxCal. Radiocarbon 43 (2A), 355–363.

Chapron, E., Beck, C., Pourchet, M., Deconinck, J.F., 1999. 1822 Earthquake triggered homogenite in Lake Le Bourget (NW Alps). Terra Nova 11, 86–92.

Cysat, R., 1601. Collectanea Chronica und denkwürdige Sachen pro Chronica Lucernensi et Helvetiae. In: Schmid, J. (Ed.), Quellen und Forschungen zur Kulturgeschichte von Luzern und der Innerschweiz, vol. 1. Diebold Schilling Verlag, Luzern, pp. 882–888.

Davenport, C., 1994. Geotechnical consequences of ground motion: hazard perspectives. Geol. Mijnb. 73, 339–356.

Deichmann, N., Ballarin Dolfin, D., Kastrup, U., 2000. Seismizität in der Nord und Zentralschweiz. Nagra, Technischer Bericht. 93 pp.

Fäh, D., Giardini, D., Bay, F., Bernardi, F., Braunmiller, J., Deichmann, N., Furrer, M., Gantner, L., Gisler, M., Isenegger, D., Jiminez, M.J., Kästli, P., Koglin, R., Masciardi, V., Rutz, M., Scheidegger, C., Schibler, R., Schorlemmer, D., Schwarz-Zanetti, G., Steimen, S., Sellami, S., Wiemer, S., Wössner, J., 2003. Earthquake Catalogue of Switzerland (ECOS) and the related macroseismic database. Eclogae Geol. Helv. 96 (2), 219–236.

Galli, P., Ferelli, L., 1995. A methodological approach for historical liquefaction research. In: Serva, L., Slemmons, D.B. (Eds.), Perspectives in Paleoseismology, Assoc. Eng. Geol., Spec. Publ., vol. 6, pp. 35–48.

Hajdas, I., Ivy, S.D., Beer, J., Bonani, B., Imboden, D., Lotter, A.F., Sturm, M., Suter, M., 1993. AMS radiocarbon dating and varve chronology of Lake Soppensee: 6,000 to 12,000 ^{14}C years BP. Clim. Dyn. 9, 107–116.

Heer, G., 1975. Aus der Vergangenheit von Kloster und Tal Engelberg 1120–1970. Verlag Benediktinerkloster Engelberg, Engelberg.

Hibsch, C., Alvarado, A., Yepes, H., Perez, V.H., Sébrier, M., 1997. Holocene liquefaction and soft-sediment deformation in Quito (Ecuador): a paleoseismic history recorded in lacustrine sediments. J. Geodyn. 24, 259–280.

Kelts, K., 1978. Geological and sedimentary evolution of Lakes Zurich and Zug. PhD thesis, ETH Zürich, Zürich. 250 pp.

Kelts, K., Briegel, U., Ghilardi, K., Hsü, K.J., 1986. The limnogeology–ETH coring system, Schweiz. Z. Hydrol. 48, 104–115.

Lemeille, F., Cushing, M.E., Carbon, D., Grellet, B., Bitterli, T., Fléhoc, C., Innocent, C., 1999. Co-seismic ruptures and deformations recorded by speleothems in the epicentral zone of the Basel earthquake. Geodin. Acta 12, 179–191.

Lotter, A.F., Sturm, M., Terranes, J.L., Wehrli, B., 1997. Varve formation since 1885 and high resolution varve analysis in hypertrophic Baldeggersee (Switzerland). Aquat. Sci. 59, 304–325.

Marco, S., Stein, M., Agnon, A., 1996. Long term earthquake clustering: a 50,000-year paleoseismic record in the Dead Sea Graben. J. Geophys. Res. 101, 6179–6191.

Mayer-Rosa, D., Cadiot, B., 1979. A review of the 1356 Basel earthquake. Tectonophysics 53, 325–333.

Meghraoui, M., Delouis, B., Ferry, M., Giardini, D., Huggenberger, P., Spottke, I., Granet, M., 2001. Active normal faulting in the Upper Rhine Graben and paleoseismic identification of the 1356 Basel earthquake. Science 293, 2070–2073.

Ming, H., 1991. Bürglen-Kaiserstuhl von Damals bis Heute. Küchler-Verlag, Giswil.

Moretti, M., Alfaro, P., Caselles, O., Canas, J.A., 1999. Modelling seismites with a digital shaking table. Tectonophysics 304, 369–383.

Neue Zürcher Zeitung (NZZ), 16.3.1964.

Obermeier, S.F., 1996. Use of liquefaction-induced features for paleoseismic analysis—an overview of how seismic liquefaction

features can be distinguished from other features and how their regional distribution and properties of source sediment can be used to infer the location and strength of Holocene paleoearthquakes. Eng. Geol. 44, 1–76.

Papastamatiou, D., 1983. Field report of an earthquake in Renaissance Europe (1601). Bull. Seismol. Soc. Am. 73/4, 1243–1251.

Pfister, C., 1999. Wetternachhersage-500 Jahre Klimavariationen und Naturkatastrophen. Verlag Paul Haupt, Bern. 304 pp.

Pfister, C., Hächler, S., 1991. Überschwemmungskatastrophen im Schweizer Alpenraum seit dem Spätmittelalter. Raum-zeitliche Rekonstruktion von Schadenmustern auf der Basis historischer Quellen. In: Glaser, R., Walsch, R. (Eds.), Historische Klimatologie in verschiedenen Klimazonen. Würzburger Geographische Arbeiten, vol. 80. Selbstverlag des Instituts für Geographie der Universität Würzburg, Würzburg, pp. 127–148.

Ricci Lucchi, F., 1995. Sedimentological indicators of paleoseismicity. In: Serva, L., Slemmons, D.B. (Eds.), Perspectives in Paleoseismology, Assoc. Eng. Geol., Spec. Publ., vol. 6, pp. 7–17.

Ringrose, P.S., 1989. Paleoseismic (?) liquefaction event in late Quaternary lake sediment at Glen Roy, Scotland. Terra Nova 1, 57–62.

Rodriguez Pascua, M.A., Calvo, J.P., De Vicente, G., Gomez-Gras, D., 2000. Soft-sediment deformation structures interpreted as seismites in lacustrine sediments of the Prebetic Zone, SE Spain, and their potential use as indicators of earthquake magnitudes during the late Miocene. Sediment. Geol. 135, 117–135.

Rodriguez Pascua, M.A., De Vicente, G., Calvo, J.P., Perez-Lopez, R., 2003. Similarities between recent seismic activity and paleoseismites during the Late Miocene in the external Betic Chain (Spain): relationship by '*b*' value and the fractal dimension. J. Struct. Geol. 25, 749–763.

Schindler, C., 1980. Geologisch–geotechnische Voruntersuchungen der N8 zwischen Sarnen und dem Brüningpass. Strasse Verk. 5, 1–6.

Schnellmann, M., Anselmetti, F.S., Giardini, D., McKenzie, J.A., Ward, S.N., 2002. Prehistoric earthquake history revealed by lacustrine slump deposits. Geology 30/12, 1131–1134.

Schwarz-Zanetti, G., Deichmann, N., Fäh, D., Giardini, D., Jimenez, J., Masciadri, V., Schibler, R., Schnellmann, M., 2003. The earthquake in Unterwalden on September 18, 1601—a historico-critical macroseismic evaluation. Eclogae Geol. Helv. 96, 441–450.

Seilacher, A., 1969. Fault-graded beds interpreted as seismites. Sedimentology 13, 155–159.

Shilts, W.W., Clague, J.J., 1992. Documentation of earthquake-induced disturbance of lake sediments using subbottom acoustic profiling. Can. J. Earth Sci. 29, 1018–1042.

Siegenthaler, C., Sturm, M., 1991. Die Häufigkeit von Ablagerungen extremer Reuss-Hochwasser. Die Sedimentationsgeschichte im Urnersee seit dem Mittelalter. Mitt. Bundesamt f. Wasserwirtschaft 4, 127–139.

Siegenthaler, C., Finger, W., Kelts, K., Wang, S., 1987. Earthquake and seiche deposits in Lake Lucerne, Switzerland. Eclogae Geol. Helv. 80, 241–260.

Sims, J.D., 1973. Earthquake-induced structures in sediments of Van Norman Lake, San Fernando, California. Science 182, 161–163.

Sims, J.D., 1975. Determining earthquake recurrence intervals from deformational structures in young lacustrine sediments. Tectonophysics 29, 141–152.

Stuiver, M., Reimer, P.J., Bard, E., Beck, J.W., Burr, G.S., Hughen, K.A., Kromer, B., McCormac, F.G., Pflicht, J.V.D., Spurk, M., 1998. INTCAL98 radiocarbon age calibration, 24,000–0 cal BP. Radiocarbon 40, 1041–1083.

Swiss Seismological Service, 2002. ECOS—Earthquake Catalog of Switzerland. ECOS Report to PEGASOS, Version 31. 3. 2002. SED, Zürich.

Theiler, A., Monecke, K., Anselmetti, F., 2003. Frequency of strong rainfall events during the Holocene recorded in lake sediments from Seelisberger Seeli in central Switzerland. 3rd International Limnogeology Congress Abstr. Vol. 294.

Weaver, J.D., Jeffcoat, R.E., 1978. Carbonate ball and pillow structures. Geol. Mag. 115, 245–253.